

EXPERIMENTAL AND THEORETICAL CHARACTERISATION OF JOSEPHSON SELF-COUPPLING IN SUB-TERAHERTZ FLUX-FLOW OSCILLATOR

D. R. Gulevich¹, P. N. Dmitriev², V. P. Koshelets², F. V. Kusmartsev¹

¹Department of Physics, Loughborough University, United Kingdom

²Kotel'nikov Institute of Radio Engineering and Electronics,
RAS, Moscow, 125009, Russia

PACS 85.25.Cp, 74.50.+r, 07.57.Hm

We present experimental and numerical results for a flux flow oscillator based on superconducting Josephson junctions. Our computationally efficient theoretical model takes into account Josephson self-coupling of the flux flow oscillator and is in a good agreement with our experimental results and previous studies.

Keywords: flux flow oscillator, superconducting Josephson junctions, fluxons, Terahertz radiation.

1. Introduction

Flux-flow oscillator (FFO) [1] is a long Josephson junction where the flux of Josephson vortices (fluxons) excite linear modes of electromagnetic waves. Typically, a length of a FFO is made considerably longer than the Josephson penetration length in order to accommodate a chain of fluxons. Because of its potential to be used as source of Terahertz and sub-Terahertz waves [2], it has attracted considerable attention from the scientific community. Investigation of FFO under the influence of different conditions such as noise and inhomogeneous bias has been done in a range of experimental [2–4] and theoretical [5–8] studies. It has been shown that fluxons in the long Josephson junction exhibit a rich behavior which is not limited to a one-dimensional fluxon motion, but involves a range of essentially two-dimensional effects [9], including excitation of the transverse modes [10]. In order to investigate the influence of two-dimensional modes on the dynamics of fluxons in a FFO, a reliable theoretical model is needed which would take into account the Josephson self-coupling effect [11] and would be efficient enough to be generalized to a model of a two-dimensional FFO which requires substantial computational resources. Here, we present our studies of the conventional FFO before proceeding to the investigation of two-dimensional effects.

2. Experimental results

Design of the harmonic mixer and all matching circuits was similar to the traditional one that was successfully used for FFO linewidth measurements (see for details [2, 3] and [4]). Current-voltage characteristics (IVCs) of the FFO measured at different magnetic fields are presented in Figure 1a. The level of the microwave power delivered to SIS matched to FFO is presented by color palette (blue corresponds to no power, red marks regions where induces by FFO SIS current exceeds 25 per cent of the quasi-particle SIS jump, see Fig. 1b). Note that the frequency of the FFO is determined by its voltage according to the Josephson relation. One can see that both SIS and FFO demonstrate perfect tunnel junction behavior with small leakage current and “0” return current of the FFO at large magnetic fields. The FFO provides enough

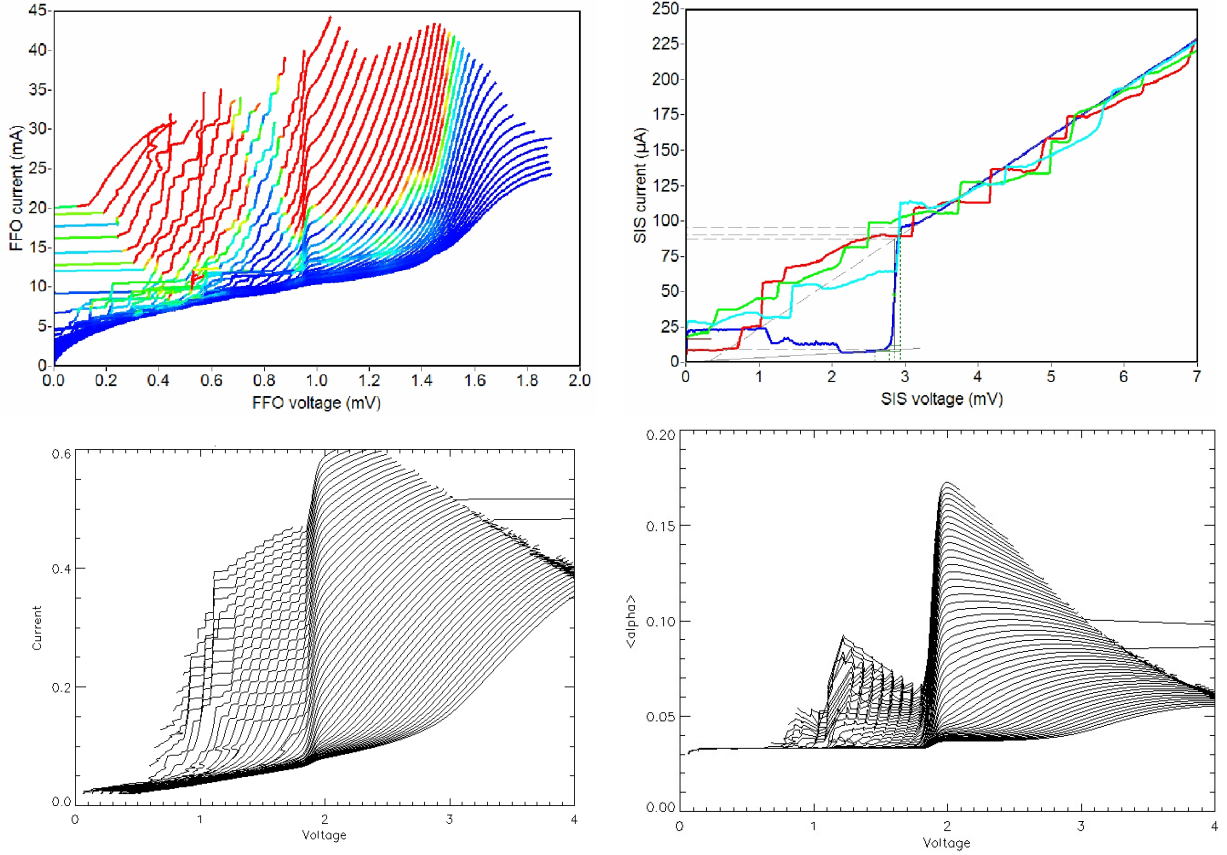


FIG. 1. (a) Experimental IVCs of the FFO measured at different magnetic fields created by current applied to integrated control line. (b) IVC of the SIS mixer: Blue – autonomous; Red, green and cyan – pumped by the FFO at frequencies 500, 600 and 700 GHz correspondingly. Note that the Josephson steps are very sharp and prominent. Positions of the steps exactly correspond to the FFO frequency. (c) Numerical IVC for FFO according to the model described in the text. The axes are normalized voltage v_{dc} and bias current γ . Different lines correspond to different values of the magnetic field h starting from 1.4 (top) to 4.0 (bottom) with the step 0.05. (d) Dependence of average damping $\langle\alpha\rangle$ versus voltage in our numerical model. Different lines correspond to different values of the magnetic field h starting from 1.4 (top) to 4.0 (bottom) with the step 0.05. Steps corresponding to one- two- and three-quanta transitions occurring at $v_g/3 = 1.9$, $v_g/5 = 1.14$ and $v_g/7 \approx 0.81$ are clearly visible. Four-quanta transition step at $v_g/9 \approx 0.63$ may also be identified for some values of magnetic field.

power to pump SIS in the design frequency range 400-750 GHz (0.8-1.5 mV). Furthermore, narrowband radiation has been measured, as in the previous experimental studies [3].

3. Numerical model

To describe FFO, we use a model of a long Josephson junction [12] with x -dependent damping parameter $\alpha(x)$,

$$\varphi_{tt} + \alpha(x)\varphi_t - \varphi_{xx} - \beta\varphi_{xxt} + \sin\varphi - \gamma = 0 \quad (1)$$

with the boundary conditions $\varphi_x(0, t) = \varphi_x(L, t) = h$ and homogeneous bias current γ . In a general case, the dependence of the bias current on x would be defined by the experimental implementation of the system. Our choice of neglecting the x -dependence is justified by our interest in universal phenomena, in a FFO rather than those related to a specific implementation. Nevertheless, the generalization to the x -dependent bias current $\gamma = \gamma(x)$ is straightforward and will not affect the computation time of the numerical scheme implemented here. The damping parameter $\alpha(x)$ in eq. (1) is subjected to Josephson self-coupling (JSC) [11]. JSC arises as a result of assisted quantum tunneling of quasiparticles in the presence of an AC field. We take this effect into account by using a damping parameter which is related to the amplitude of the AC field at a each point of the junction, $\alpha(x) = \gamma_{qp}/v_{dc}$ with [13]

$$\gamma_{qp} = \sum_{n=-\infty}^{n=\infty} J_n^2\left(\frac{v_{ac}}{2\omega}\right) \gamma_{dc}(v_{dc} + 2n\omega), \quad (2)$$

where v_{dc} and v_{ac} are normalized DC and AC voltages: $v_{dc} = 2eV_{dc}/\hbar\omega_p$, $v_{ac} = 2eV_{ac}/\hbar\omega_p$, ω is normalized to the plasma frequency ω_p , J_n are Bessel functions and $\gamma_{dc}(v)$ is modelled by

$$\gamma_{dc}(v) = \alpha_0 v \left(1 + b \frac{(v/v_g)^p}{1 + (v/v_g)^p} \right).$$

We took values of the parameters $b = 35$, power index $p = 80$, and gap voltage $v_g = 5.7$ to be consistent with the model used in [8]. Also, for the sake of consistency with the previous study [8], the length of the FFO was taken to be $L = 40$ Josephson penetration lengths, damping parameters $\alpha_0 = 0.033$ and $\beta = 0.035$. As it is reasonable to assume that self-coupling of FFO is dominated by a single harmonic the DC and AC components can be found by approximations

$$v_{dc} = \langle \dot{\varphi} \rangle \quad \text{and} \quad v_{ac} = \frac{1}{2} (\max \dot{\varphi} - \min \dot{\varphi}),$$

which save much of the computational time as compared to finding of the amplitudes with the fast Fourier transform. Equation (1) was solved numerically by the explicit finite difference scheme at fixed function $\alpha(x)$. The self-consistent $\alpha(x)$ has been found by an iterative procedure until the desired accuracy in $\alpha(x)$ is reached. The number of discrete points along X was 200, the time step and the integration time were varied in accordance with the specific choice of parameters. The code has been written in IDL programming language widely used in astronomy applications [14]. The results of our numerical simulations are presented on Fig. 1c and are in qualitative agreement with our experimental results on Fig. 1a and earlier numerical studies [6–8].

The slopes of the IVC curves differ slightly from the experimental results at high values of the bias current. This can possibly be attributed to the fact that we have used ideal, non-radiative boundary conditions, while in the experimental system, a certain amount of the radiation power may escape through the boundary, causing the IVC curves to bend up as seen on the experimental graph 1a. Fig. 1d shows our numerical results for the dependence on voltage of the average damping parameter defined as:

$$\langle \alpha \rangle = \frac{1}{L} \int_0^L \alpha(x) dx$$

Distribution of the AC amplitude v_{ac} and the distribution of the damping parameter α along the FFO is shown on Fig. 2a,c and 2b,d for two different sets of values for magnetic field and bias current. The spectrum of frequencies at the FFO's left boundary is shown on Fig. 2e and f. At certain regimes the spectrum becomes sophisticated with more harmonics turning up like on Fig. 2f. In this case, although the dependence of the spectrum on the choice of the

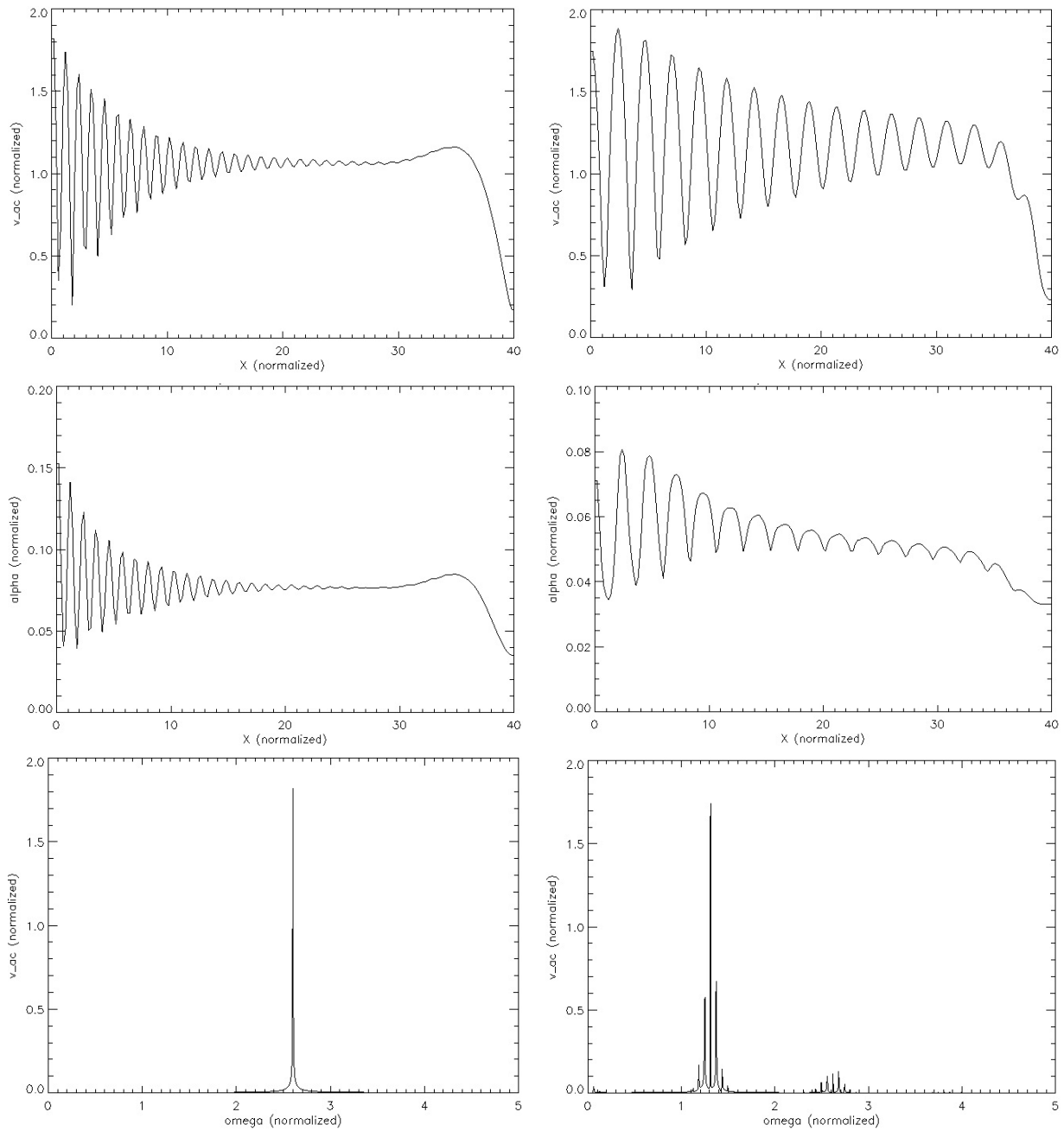


FIG. 2. (a), (b) - distribution of the amplitude of AC drive v_{ac} on the main harmonics $\omega = v_{dc}$ along the FFO; (c), (d) - distribution of damping parameter in the FFO; (e), (f) - frequency spectrum at the FFO's left boundary; X axis is normalized frequency and Y axis shows v_{ac} . Calculations were performed for two set of parameters: $h = 3.0$, $\gamma = 0.3$ (a,c,e) and $h = 2.0$, $\gamma = 0.2$ (b,d,f), correspondingly.

calculation parameters, such as time step and maximum integration time, has not been observed, the influence of a numerical artifact may not be completely excluded.

4. Conclusion

To summarize, we have presented a theoretical model which is consistent with our experimental results and previous theoretical studies. The model is numerically efficient, and therefore, has the potential to be generalized for the study of the rich two-dimensional dynamics of magnetic flux in two-dimensional FFOs.

Acknowledgements

The work was supported by the RFBR and the Ministry of Education and Science of the Russian Federation.

References

- [1] T. Nagatsuma et al. *J. Appl. Phys.*, **54**, 3302 (1983); *ibid* **56**, 3284 (1984); *ibid* **58**, 441 (1985); *ibid* **63**, 1130 (1988).
- [2] V. P. Koshelets and S. V. Shitov. *Supercond. Sci. Technol.*, **13**, R53 (2000).
- [3] V. P. Koshelets et al. *Supercond. Sci. Technol.*, **17**, S127 (2004); V. P. Koshelets et al. *IEEE Trans. Appl. Supercond.*, **17**, 336 (2007); M. Yu. Torgashin et al. *IEEE Trans. Appl. Supercond.*, **17**, 339 (2007).
- [4] IRE RAS Lab. of Supercond. Devices web page, <http://www.cplire.ru/html/lab234/publications.htm>.
- [5] E. A. Matrozova, A. L. Pankratov and L. S. Revin. *J. Appl. Phys.*, **112**, 053905 (2012); L. S. Revin and A. L. Pankratov. *Phys. Rev. B*, **86**, 054501 (2012); E. A. Matrozova et al. *J. Appl. Phys.*, **110**, 053922 (2011); A. L. Pankratov. *Phys. Rev. B*, **78**, 024515 (2008); A. L. Pankratov et al. *J. Phys.: Conf. Ser.*, **97**, 012303 (2008); A. L. Pankratov, V. L. Vaks and V. P. Koshelets. *J. Appl. Phys.*, **102**, 063912 (2007).
- [6] A. S. Sobolev, A. L. Pankratov, and J. Mygind. *Physica C*, 435, 112 (2006).
- [7] M. Jaworski. *Phys. Rev. B*, **81**, 224517 (2010).
- [8] A. L. Pankratov, A. S. Sobolev, V. P. Koshelets, and J. Mygind. *Phys. Rev. B*, **75**, 184516 (2007).
- [9] K. Nakajima et al. *J. Appl. Phys.*, **47**, 1620 (1976); D. R. Gulevich and F. V. Kusmartsev. *Phys. Rev. Lett.*, **97**, 017004 (2006); D. R. Gulevich and F. V. Kusmartsev. *Supercond. Sci. Tech.*, **20**, S60 (2007); D. R. Gulevich and F. V. Kusmartsev. *New J. Phys.*, **9**, 59 (2007); D.R. Gulevich et al. *Physica C*, **468**, 1903 (2008); D. R. Gulevich et al. *J. Appl. Phys.*, **104**, 064507 (2008); H. Farhan-Hassan et al. Flux-Flow Oscillator (FFO) Made with the Fluxon Cloning Circuits. *Terahertz and Mid Infrared Radiation*, p. 29, Springer (2011).
- [10] D. R. Gulevich et al. *Phys. Rev. Lett.*, **101**, 127002 (2008); D. R. Gulevich et al. *Phys. Rev. B*, **80**, 094509 (2009).
- [11] N.R. Werthamer. *Phys. Rev.*, **147**, 255 (1966); L.-E. Hasselberg, M.T. Levinsen, and M.R. Samuelsen. *Phys. Rev. B*, **9**, 3757 (1974); V.P. Koshelets, et al. *Phys. Rev. B*, **56**, 5572 (1997).
- [12] K. K. Likharev. *Dynamics of Josephson Junctions and Circuits*. Gordon and Breach, New York, 1986. A. Barone and G. Paterno. *Physics and Applications of the Josephson Effect*, Wiley, New York, 1982.
- [13] J. R. Tucker. *IEEE Journal of Quantum Electronics*, **15**, 1234 (1979); J. R. Tucker and M. J. Feldman. *Rev. Mod. Phys.*, **57**, 1055 (1985).
- [14] Interactive Data Language (IDL): <http://www.itlvis.com> and <http://idlastro.gsfc.nasa.gov>.